A force measurement instrument for optical tweezers based on the detection of light momentum changes

Arnau Farré*[a,b], Ferran Marsà[a,b], Mario Montes-Usategui[a,b]
[a]Impetux Optics, Trias i Giró 15 1-5, 08034 Barcelona, Spain; [b]Optical Trapping Lab – Grup de Biofotònica, Departament de Física Aplicada i Òptica, Universitat de Barcelona, Martí i Franquès 1, 08028 Barcelona, Spain

ABSTRACT

In this work, we present and discuss several developments implemented in an instrument that uses the detection of the light momentum change for measuring forces in an optical trap. A system based on this principle provides a direct determination of this magnitude regardless of the positional response of the sample under the effect of an external force, and it is therefore to be preferred when *in situ* calibrations of the trap stiffness are not attainable or are difficult to achieve. The possibility to obtain this information without relying upon a harmonic model of the force is more general and can be used in a wider range of situations. Forces can be measured on non-spherical samples or non-Gaussian beams, on complex and changing environments, such as the interior of cells, or on samples with unknown properties (size, viscosity, etc.). However, the practical implementation of the method entails some difficulties due to the strict conditions in the design and operation of an instrument based on this method. We have focused on some particularly conflicting points. We developed a process and a mechanism to determine and systematically set the correct axial position of the device. We further analyzed and corrected the non-uniform transmittance of the optical system and we finally compensated for the variations in the sensor responsivity with temperature. With all these improvements, we obtained an accuracy of ~5% in force measurements for samples of different kinds.

Keywords: Optical trapping, optical tweezers, optical manipulation, back-focal-plane interferometry, force calibration

1. INTRODUCTION

Since proposed in the late 1990s[1, 2], back-focal-plane interferometry has found an increasing acceptance for nanometer-precision measurements of displacements of trapped samples. This has been the preferred choice for many studies, particularly, because of the large attainable temporal bandwidth (up to megahertz) and due to its natural capability of detecting relative displacements of the particle instead of absolute movements. This cheaper solution has rapidly replaced video imaging for tracking the sample motion when precision was a concern. Combined with force calibration through, for example, the power spectrum analysis of the sample's thermal motion, the technique offers the possibility to determine forces in the piconewton range.

We recently showed[3, 4] that an optimized back-focal-plane interferometry can be used to directly track the rate of momentum transfer between sample and beam to thus determine the force without an *in situ* calibration. This approach, originally proposed and developed by S. Smith *et al.* for counter-propagating traps[5], relies upon measuring the deflection of the laser when it interacts with the trapped object. The deviation of the beam is a measure of the change of the light momentum in units of nP/c (where n is the refractive index of the medium, P the laser power and c the light velocity in vacuum), so it is hence univocally connected to the optical force through a factor independent of the sample properties.

A back-focal-plane interferometry instrument is a suitable system for measuring both the beam deflection and the laser power at the sample. The advantage of this method is that the force measured from first principles (by measuring the amount of momentum transferred to the sample and thus how much is deflected) does not require a calibration before every experiment. Thus, with a single thorough calibration of the conversion between deflections and voltages, the probability of introducing errors in each experiment is greatly reduced, enhancing the final precision. In addition, the measurement of macroscopic parameters, such as the transmittance of the collecting optics or the focal length of the system is less sensitive to errors and produces therefore a more accurate outcome.

*arnau.farre@impetux.com; www.impetux.com

However, the strength of this approach is not only the quality of the measurements but the possibility to perform experiments which are otherwise complicate or impossible to do and which greatly expand the capabilities of optical trapping. Some examples are the measurement of forces with non-spherical particles, with arbitrarily-shaped traps generated with digital holography, for example, or inside complex environments such as cells.

The main difference with a conventional back-focal-plane interferometry is that the accurate detection of the light momentum requires some strict experimental requisites on the setup, detailed in Ref. 3, which make the practical implementation of the method difficult. Here, we present and discuss some developments included in a new force sensor to guarantee that the conditions are correctly fulfilled in practice and that therefore a constant and permanent force calibration is achieved during the routine operation.

2. EXPERIMENTAL SETUP

The optical trapping system used in these experiments was based on a commercial microscope (*Nikon*, TE2000-E). A TEM_{00} infrared laser (1064 nm, *IPG Photonics*, YLM-5-1064-LP) was expanded to slightly overfill the back aperture of a water-immersion objective (*Nikon*, CFI Plan Apo VC 60xA WI, NA = 1.2), simultaneously used to observe the sample and to focus the beam to a tiny spot (~1 μm) and create thus the optical trap. The measurement of forces was achieved by means of the developed detection system (Fig. 1).

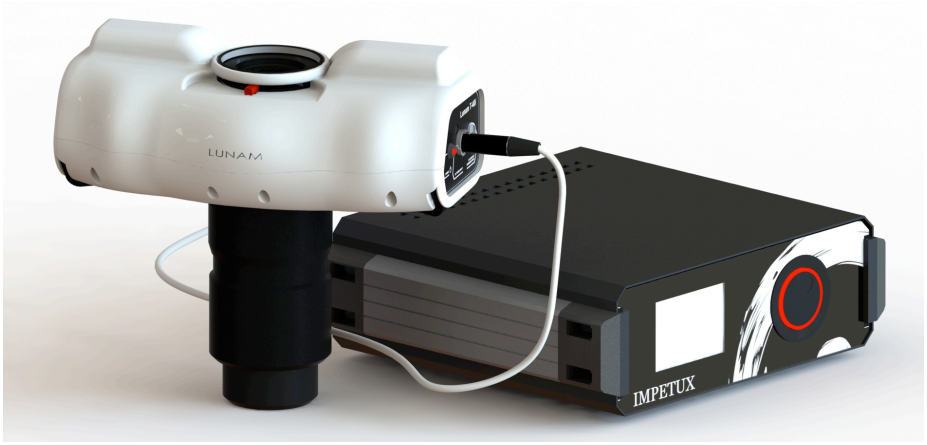

Figure 1. Image of the developed force sensor based on the detection of the light momentum change. Both the sensor head and its power supply are displayed.

When a specimen is trapped and an external force is applied on it, the beam in whole is deflected as a response of the momentum transferred to the light. The detection instrument captures this light and extracts the force information from the analysis of the deviation of the beam with a position photodiode. An optical equivalent of the back focal plane (BFP) of the collecting lens is formed onto the detector plane, so intensity shifts of the far-field distribution of the collected light are converted by the detector into momentum measurements in units of volts, and further translated into piconewtons after an absolute calibration of the whole system.

There are two main parameters involved in the conversion of the output signal into deflections of the beam and ultimately on force measurements[4, 5]. One of the magnitudes to be determined is the amount of energy interacting with the particle. In this case, the product of the transmittance of the system, T, and the detector responsivity, $\Re_\lambda$, at a wavelength λ provides the conversion from volts to watts. This calibration can be used to know the laser power used during an experiment. The second important factor is the focal length of the instrument, f',which fixes the conversion from changes in the mean direction of propagation of the beam at the sample to shifts, x', of the light pattern on the detector plane (Fig. 2). If the optical design of the system fulfills the Abbe sine condition ($x' = f'n\sin\theta$), then, the force, F, and the output voltage, V, are related through the following equation:

$$F_x = \frac{R_D^x}{\Re_\lambda Tcf'} V_x \tag{1}$$

The conversion factor also depends on the detector radius, R_D, since the signal is proportional to the intensity shifts normalized by the size of the sensitive area of the photodiode.

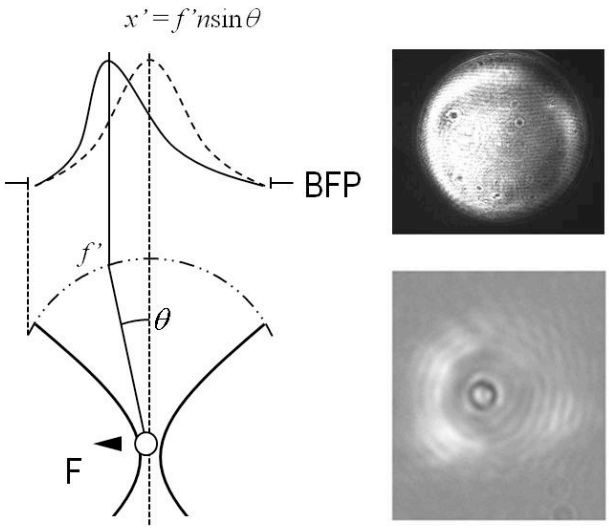

Figure 2. Scheme of the detection process. Scattering of the trapping laser by a particle is seen as a deflection of the beam (bottom) and ultimately as a shift in the intensity distribution at the BFP of the collecting lens (top). The light pattern is converted into a measurable quantity by a position sensitive detector, which records the changes in *x'* and provides direct measurements of the force once calibrated.

3. RESULTS

3.1 Instrument's axial position

The cornerstone of the practical implementation of the method is the capture of a significant fraction of the light scattered by the sample. The loss of information about the rate of momentum transfer between light and particle can lead to an underestimation of the applied force, eventually making the system only valid for tracking the sample displacements[2, 4].

A constant calibration can be achieved under some conditions: essentially, using a collecting lens with a numerical aperture, NA, larger than the refractive index of the suspension medium, n, and trapping the sample within a region of thickness $h < 100\ \mu$m below the upper glass of the microchamber[3] (Fig. 3).

When the instrument is correctly designed and set, the amount of scattered light collected and analyzed by the system is close to the total power of the beam, despite of using a single lens for this. The results show that even in the most unfavorable case, corresponding to particles with sizes close to the laser wavelength, backscattering represents only a 2-3% of the total beam, in agreement with theoretical results (Fig. 3). For larger particles (some microns), the reflection, given by $(n - n')^2/(n + n')^2$ since the hitting rays are almost perpendicular to the particle surface for a significant range of sample displacements (n and n' being the refractive indexes of the medium and the sample, respectively), represents a smaller fraction of the whole beam (typically < 1%). For smaller objects (some hundreds of nanometers), the amount of scattered light radiated in a 4π solid angle, and therefore in the backward direction, usually represents less than 1%. As shown in Ref. 3, the resulting effect of this almost negligible loss of information has, in practice, a small impact.

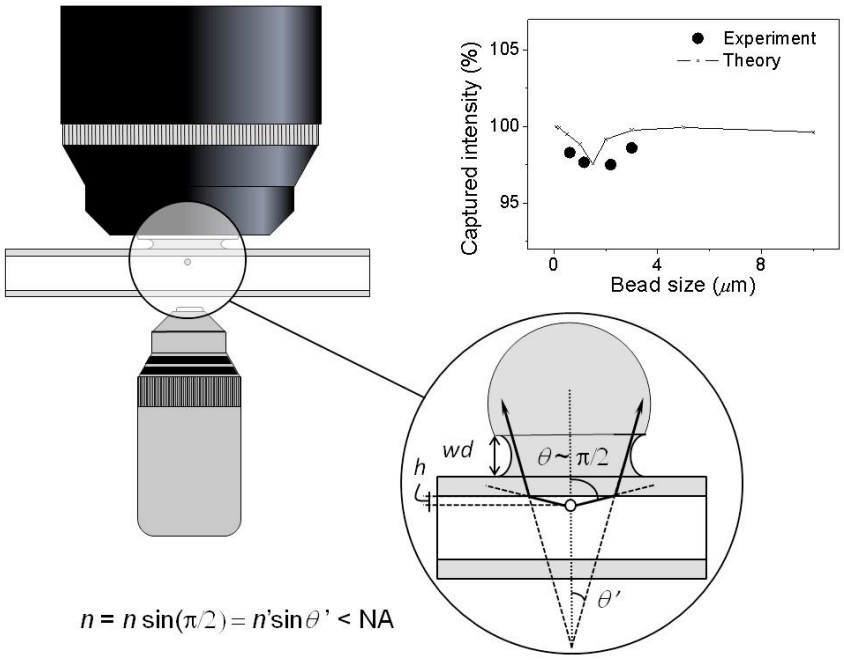

Figure 3. Scheme of the trapping configuration for a correct detection of the light momentum change.

Nevertheless, following these indications may not totally guarantee the accurate measurement of the momentum. The correct collection of the light and its further transmission towards the photodetector requires an extra effort in the design of the instrument. One of the most critical aspects is the axial positioning, *wd*, of the front lens of the detection system (Fig. 3). Even if the instrument is designed with a high-NA collecting lens, the captured beam could be a fraction of it if the front lens was not situated at the working distance. This can be observed in the light patterns recorded at the back focal plane, BFP, of the collecting lens. Figure 4 shows the intensity distribution obtained when a microsphere is held in the optical trap. In this case, two differentiated disks arise as a consequence of the scattering (outer disk) of a fraction of the incident beam[3] (inner disk). The larger diameter of the former indicates that the light re-scattered by the particle spans a larger solid angle, specifically, a full 4π sphere. The trapping objective was chosen with a low NA to make the difference clearer between the two disks.

However, when the instrument height is not set properly, the total diameter of the light pattern decreases until there is no presence of scattered light (outer disk) in the recorded intensity. Furthermore, the variation in this effective collecting solid angle of the front lens is considerably sensitive with the axial position of the system. A variation of only 1 mm can halve the NA of the lens. To avoid this problem and obtain a systematic procedure to set the instrument height we developed a specific solution. We calibrated the BFP of the collecting lens to obtain a conversion from positions in this plane and angles at the sample, so we could determine the effective solid angle of the system by analyzing the size of the light patterns to thus know the correct axial position of the system. The first step was to determine this relation.

As discussed in Ref. 3, the detection of the light momentum requires that the light pattern formed at the detector plane corresponds to the Fourier transform of the light distribution at the trapping plane, and this relation must be fulfilled across the entire plane. In order to guarantee this condition, the optical design involved in the capture and projection of the beam onto the sensor must follow the Abbe sine condition, that is, light propagating with the same angle at the sample, θ, must end up at the same position on the detector, x', given by the relation $x' = f' \cdot n \cdot \sin\theta$, where f' is the focal length of the instrument and n is the refractive index of the suspension medium.

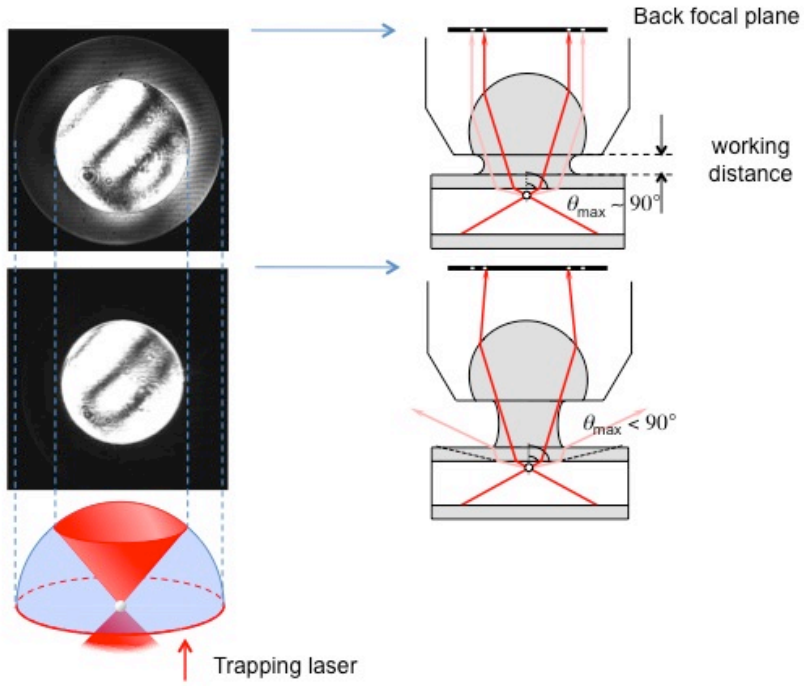

Figure 4. Effective NA of the front lens as a function of the distance between instrument and sample.

We designed the instrument to strictly follow this relation, which was used in turn to obtain the conversion between positions and angles (Fig. 5). Once this calibration was achieved, we could use the images of the intensity patterns at the detection plane to determine the amount of collected light. When the whole beam was captured by the front lens, the diameter of the light pattern was given, according to the Abbe sine condition, by $D = 2r_{max} = 2f'n\sin\theta_{max} = 2f'n$ since the maximum angle captured by the instrument was for light propagating almost parallel to the upper surface of the microchamber ($\theta_{max} \sim \pi/2$)[3]. Figure 5 shows an example of two experiments. Only in the first case, for which the diameter corresponded to an NA equal to the refractive index of the suspension medium, the system was correctly situated at the working distance.

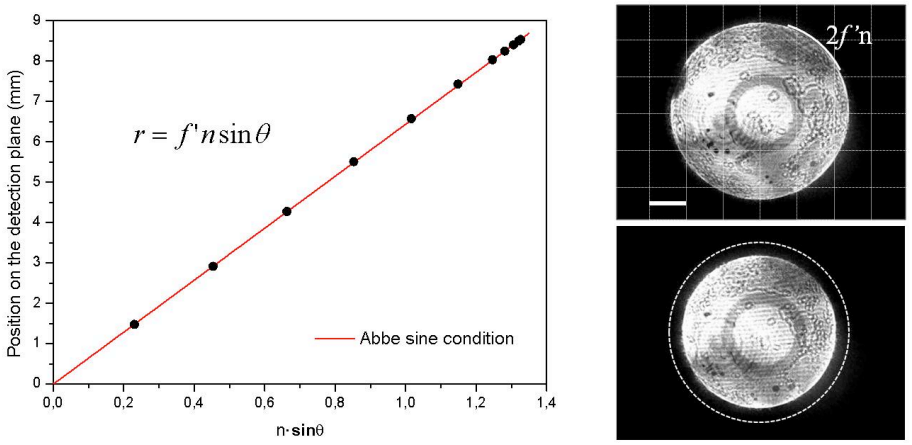

Figure 5. The calibration of the BFP of the collecting lens shows that the instrument perfectly follows the Abbe sine condition. The calibration provides a measurement of the solid angle captured by the system, which can be used to correctly set the position of the sensor. (Top) NA ~ n. (Bottom) NA < n. The scale bar corresponds to an effective NA of 0.5.

With a solid method to establish the position of the instrument, we included a mechanism to systematically and reliably set the height of the device based on the observation of a reference mark at the sample plane. An iris above the collecting lens was set at a distance so when its image was observed in sharp focus at the sample, the captured light pattern corresponded to the whole forward-scattered beam. This method enabled a repetitive setting of the instrument position without requiring the inspection of the intensity distribution recorded by the system.

3.2 Uniform transmittance

When the system is correctly set, the whole deflected beam can be captured by the front lens even for large displacements of the sample. However, as we will show next, the collection of this light is not uniform for the different angles of propagation. Due to the angular dependence of the transmittance between two media with different refractive indexes, the relative scattered intensity changes in the radial direction at the detection plane. The same small effect happens repetitively throughout the whole optical system giving rise to a large accumulated change between the center and the edges of the light pattern at the PSD. This eventually results into an underestimation of the beam deflection and an incorrect measurement of the force (Fig. 6).

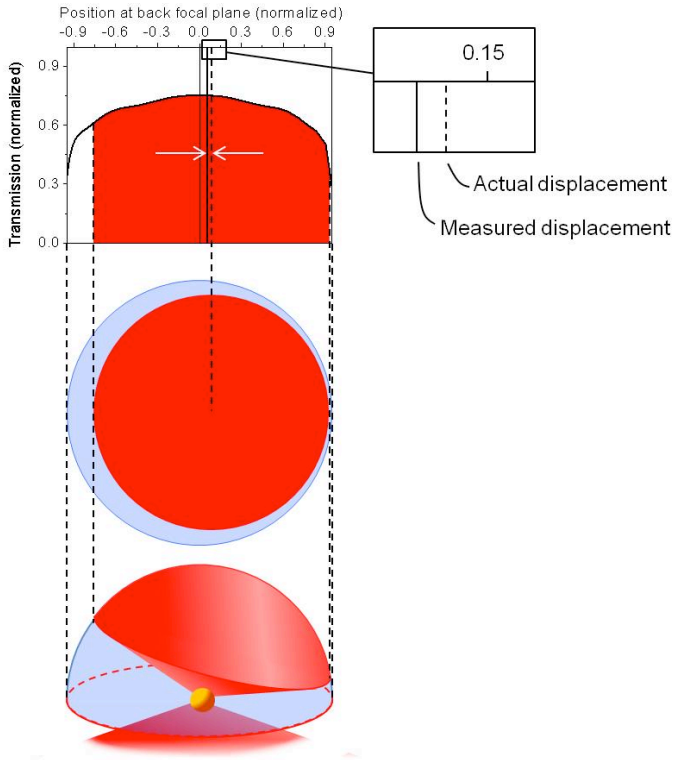

Figure 6. The non-uniform transmittance of the optical system translates into an underestimation of the deflection of the beam.

The main variation is concentrated in the front lens where larger angles show up. Its transmittance was determined in a dual-lens system by scanning the laser across the back aperture of the first lens and measuring the output power, P_{out}, at the back aperture of the second lens and determining the transmittance as (Fig. 7a):

$$T(r) = \sqrt{\frac{P_{out}(r)}{P_{in}(r)}} \tag{2}$$

where P_{in} corresponds to the incident power. The use of an expanded beam filling the entire lens with a diaphragm to control its diameter was avoided since this alternative method has been shown to overestimate the correct value of T [6].

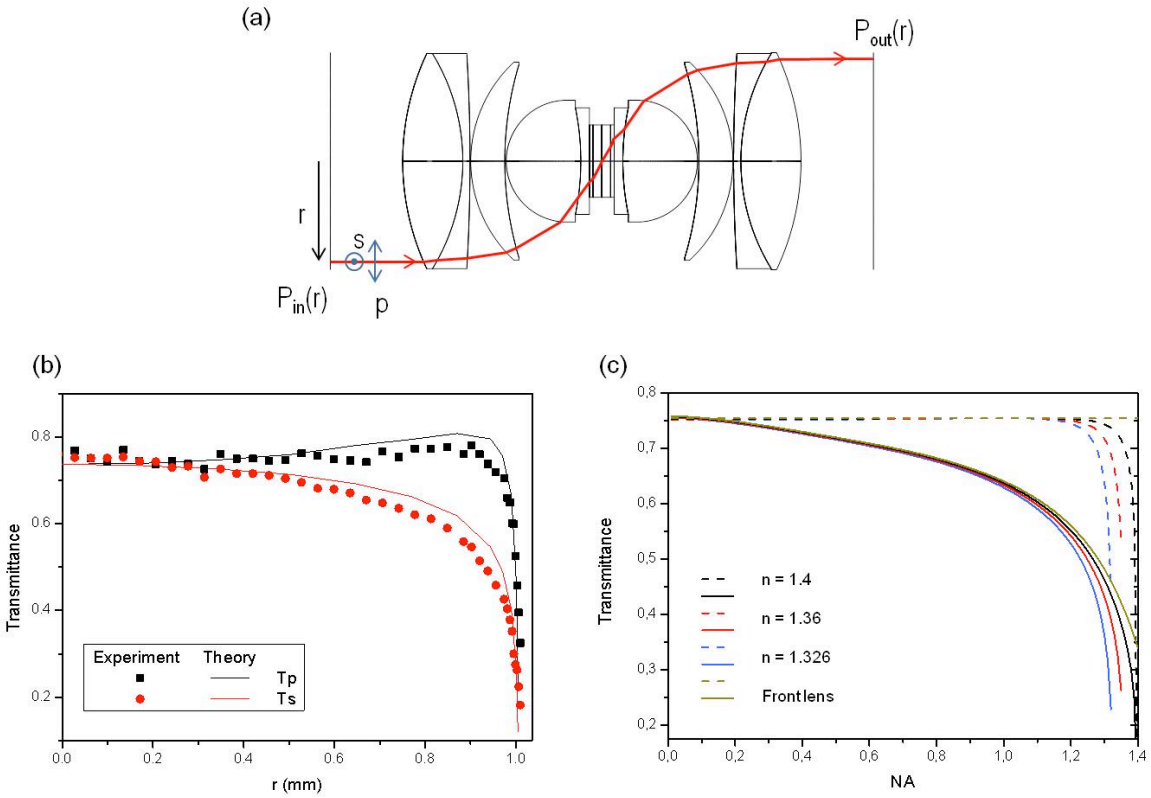

Figure 7. Calibration of the angular transmittance of the system. (a) Computer simulation of the experiment based on a dual-lens configuration. The square root of the ratio between the output and the input power gives a measurement of the transmittance. (b) Results for the s- and p- polarizations. The computer simulation provides similar results. (c) The transmittance depends on the refractive index of the suspension medium.

By repeating the same measurement at different positions, r, we determined the radial dependence of the transmittance. Different curves were obtained for the perpendicular (s) and parallel (p) polarizations. Figure 7b shows the experimental data for an infrared (1064 nm) laser. The results from a computer simulation of the system showed indeed that the added contribution of the Fresnel coefficients at the different interfaces between materials originated the strong change observed in the experiments. The small discrepancies between experiment and simulations were due to the lack of the complete information about the anti-reflection coatings of the lenses.

The transmittance T_s was found to decrease a 25% for rays propagating with an angle of 65º, corresponding to the NA of our trapping objective, 1.2. For the parallel polarization, the transmittance was barely affected for radial distances smaller than 90% of the total radius of the back aperture of the lens. Only at large angles, the transmittance dropped. This sudden change, also observed in the perpendicular component, was mainly generated at the interface between the suspension water and the glass surface of the microchamber. The theoretical curves in Fig. 7c show the effect of the refractive indexes of the suspension medium in the transmittance curve.

The consequence of this radial change in the transmittance is that, as depicted in Fig. 6, intensity shifts at the BFP underestimate the actual deflection of the beam, so detector currents are not correctly translated into force by a single

constant factor. However, even when a small force is applied and, therefore, the perturbation on the momentum reading is small, the angular variation of the transmittance leads, according to Eq. 1, to different force calibrations depending on, for example, the NA of the trapping objective.

To eliminate this artifact, we designed and built a transmission mask to compensate for the losses of light at the edges of the laser beam. The mask was placed at the BFP of the collecting lens with a mechanism to correctly center it along the directions perpendicular to the optical axis. The result is a flat and uniform transmittance throughout the whole plane (Fig. 8). The optical density of the mask was thoroughly calibrated to achieve the correct transmittance at each point. With this improvement, the intensity pattern impinging on the detector preserved the same relative structure as that scattered by the sample.

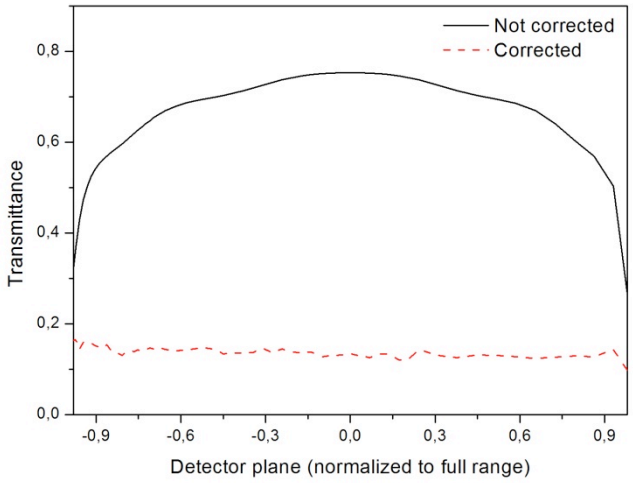

Figure 8. Experimental transmittance with and without correction mask.

Although simpler to solve, a similar effect can be introduced by the sensor itself due to a non-uniform responsivity. The detector responsivity is one of the most important parameters of the detection instrument as it measures the efficiency with which carriers are generated due to incident light, and represents, therefore, the ultimate conversion to a measurable quantity. The response may vary across the detector sensitive area, leading to variations in force calibration. The choice of a uniform response detector is an important parameter.

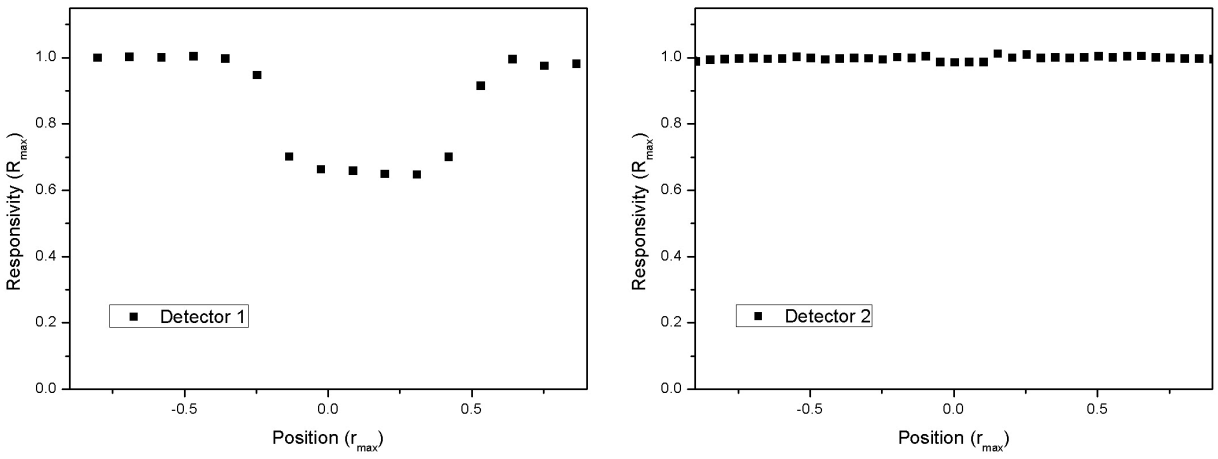

Figure 9. Detector response for two different commercial position sensitive detectors.

In Fig. 9, we can observe how low-cost sensors can show up changes in responsivity as large as 40%, which may translate into remarkable errors in the force calibration.

3.3 Temperature dependence of the force calibration

Finally, we analyzed the effect of temperature on force calibration. The sensor responsivity depends on different parameters (device material, operating wavelength, bias voltage, etc.) that remain fixed, but also upon magnitudes that can change from one experiment to another. The sensor temperature is one of these critical parameters.

For 1064 nm, this variation can reach 1-2%/ºC, which may represent a significant change if the instrument calibration does not include such dependence. We experimentally measured this effect by changing the room temperature and analyzing the variation of the sensor response to a certain laser power (Fig. 10). We found a change of 1-1.5% per Celsius degree within a range of 20-27 ºC. This can easily represent a variation of 5% during the same day if it is not taken into account. To compensate for this, we introduced a thermometer at the sensor head of the instrument to automatically adapt the force readings to the operating temperature.

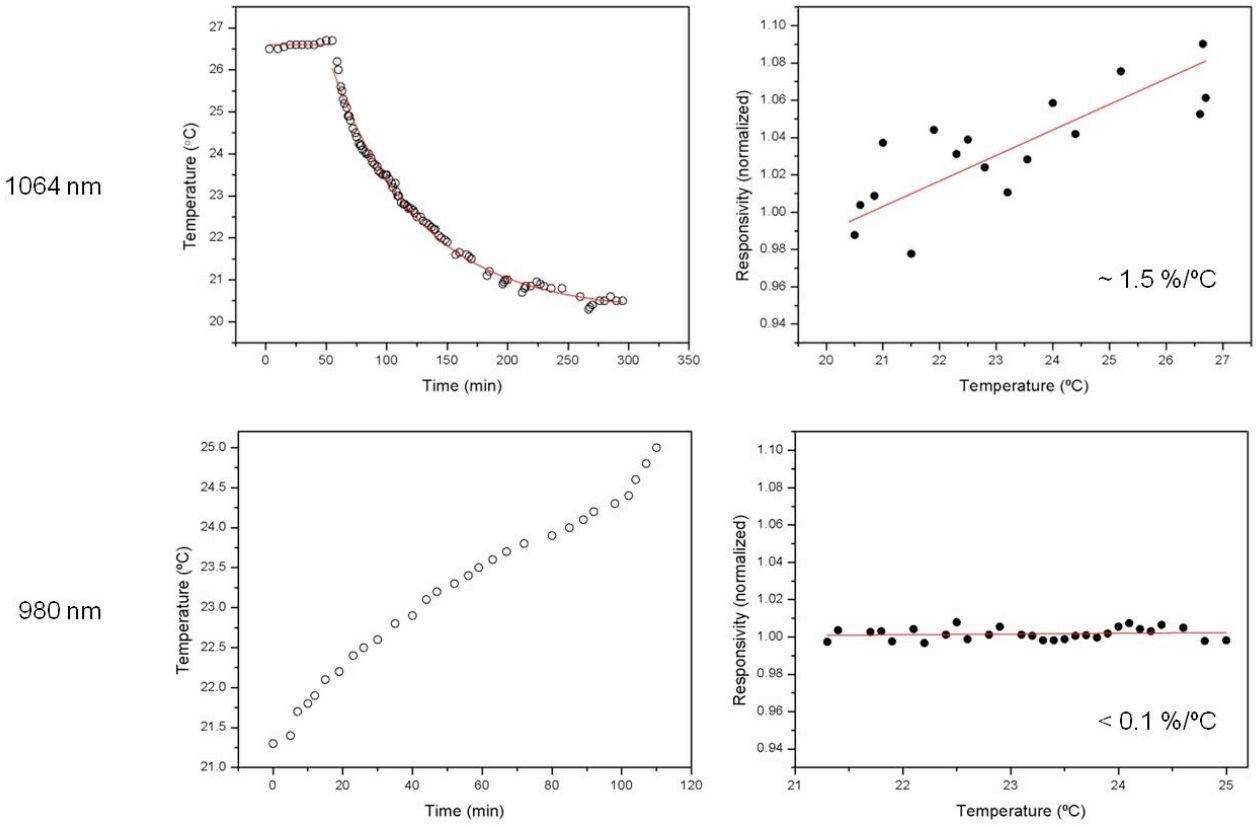

Figure 20. Variation in the detector's responsivity for different room temperatures. The change depends on the laser wavelength.

The change in responsivity depends on the laser wavelength. The same calibration was obtained for 980 nm and found almost no variation as expected (Fig. 10).

3.4 Force and position calibration

Once the different parameters of the device were calibrated, the force was directly determined by the output voltage and was therefore independent of the specific properties of the sample, such as size or shape. Figure 11 shows a typical experiment where controlled forces were applied on trapped samples and compared to the sensor output. By moving the

microchamber with a piezoelectric stage, we exerted hydrodynamic forces on microspheres with different diameters, $2R$. The magnitude of the force was tuned by changing the frequency and the amplitude of the stage oscillation. The measured forces were found to be equal to the Stokes' law, $6\pi\eta R$ (η is the medium viscosity), within a ~5% for particles of different sizes and materials. Correct measurements can be typically obtained up to the escape force of the trap.

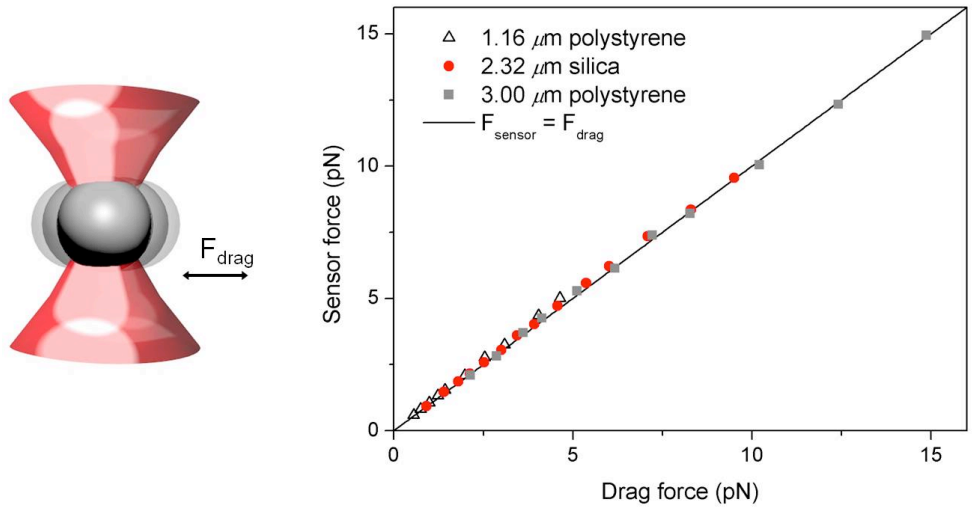

Figure 11. Experimental results show that the sensor output is equal to the drag force applied on samples of different sizes and materials.

The connection of the force with position through a linear relation guarantees the possibility of measuring displacements of the sample with the same instrument and allows a further calibration of the trap stiffness:

$$x = \frac{F_x}{\kappa} \propto V_x \tag{3}$$

Figure 12 shows a typical power spectrum of a trapped 1.87-μm polystyrene microsphere suspended in water[7]. The sampling frequency was 49 kHz. Different effects, such as aliasing, the frequency dependence of the drag coefficient or the low-pass filtering of the photodetector due to the use of an infrared laser were taken into account for the fitting of the experimental data. The spectral noise of the instrument is also shown for comparison.

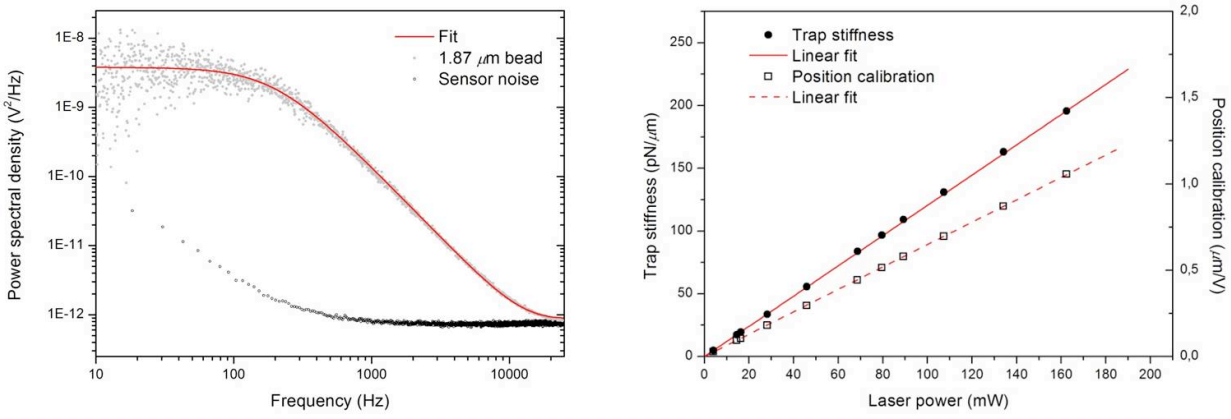

Figure 12. Power spectral density of the Brownian motion of a trapped microsphere (1.87 μm) and of the sensor noise (left). Trap stiffness and position calibration are linear with laser power once the effect of the laser heating is corrected (right).

Both the trap stiffness and the conversion from volts to microns obtained from the fitting to the experimental data show a high linearity with laser power when the heating effect of the laser was corrected[8]. Laser power measurements were obtained from the transmittance and the responsivity of the instrument calibrated before.

4. CONCLUSIONS

We pointed out different effects that must be taken into account to obtain accurate force determinations through the direct measurement of the light momentum. In particular, we showed the necessity of determining a procedure to systematically set the instrument's axial position at the same distance from the sample to collect the whole forward-scattered light. Errors of one millimeter or less can considerably change the effective NA of the front lens and lead to an underestimation of the force.

We likewise discussed the problem of a non-uniform transmittance of the collected beam, even when the detection instrument is set at a correct position. High-NA optics typically suffers from a degradation of the light transmittance at large angles due to the angular dependence of the Fresnel coefficients at the interfaces between lenses. If this effect is not compensated, the recorded change in the light momentum does not correctly describe the deflection of the beam at the sample. A similar effect is produced by a non-uniform responsivity of the photodiode. The appropriate selection of a flat-response detector is important to avoid errors in the measurement.

Finally, we analyzed the dependence of the sensor's responsivity with temperature. Changes in the room temperature during experiments can lead to variations in the total force calibration of the instrument. To eliminate this effect, the response must be calibrated for the laser wavelength used in the experiments and a thermometer at the sensor head of the instrument must be used to know the exact operating temperature.

REFERENCES

[1] Visscher, K., Gross, S. P. and Block, S. M., "Construction of multiple-beam optical traps with nanometer-resolution position sensing," IEEE J. Select. Topics Quantum Electron. 2, 1066–1076 (1996).

[2] Gittes, F. and Schmidt, C., "Interference model for back-focal-plane displacement detection in optical tweezers," Opt. Lett. 23, 7-9 (1998).

[3] Farré, A. and Montes-Usategui, M., "A force detection technique for single-beam optical traps based on direct measurement of light momentum changes," Opt. Express 18, 11955-11968 (2010).

[4] Farré, A., Marsà, F. and Montes-Usategui, M., "Optimized back-focal-plane interferometry directly measures forces of optically trapped particles," Opt. Express 20, 12270-12291 (2012).

[5] Smith, S. B., Cui, Y. and Bustamante, C., "Optical-trap force transducer that operates by direct measurement of light momentum," Methods Enzymol. 361, 134–162 (2003).

[6] N. B. Viana, M. S. Rocha, O. N. Mesquita, A. Mazolli and P. A. Maia-Neto, "Characterization of objective transmittance for optical tweezers," Appl. Opt. 45, 4263-4269 (2006).

[7] Berg-Sørensen, K. and Flyvbjerg, H., "Power spectrum analysis for optical tweezers," Rev. Sci. Instrum. 75, 594-612 (2004).

[8] E. J. G. Peterman, F. Gittes and C. F. Schmidt, "Laser-induced heating in optical traps," Biophys. J. 84, 1308-1316 (2003).